

Strangeness Production at the SPS

C. Blume, for the NA49 Collaboration*
Fachbereich Physik, J.W. Goethe-Universität,
Max-von-Laue-Str. 1, D-60438 Frankfurt am Main, GERMANY
 (Received)

Systematic studies on the production of strange hyperons and the ϕ meson as a function of beam energy and system size performed by the NA49 collaboration are discussed. Hadronic transport models fail to describe the production of multi strange particles (Ξ , Ω), while statistical models are generally in good agreement to the measured particle yields at all energies. The system size dependence is well reproduced by the core-corona approach. New data on $K^*(892)$ production are presented. The yields of these short-lived resonances are significantly below the statistical model expectation. This is in line with the interpretation that the measurable yields are reduced due to rescattering of their decay products inside the fireball.

PACS numbers: 25.75.-q

Keywords: Heavy ion reactions, quark-gluon plasma, strangeness production

I. INTRODUCTION

The production of strange particles has always been a key observable in heavy-ion reactions and its enhancement was one of the first suggested signatures for quark-gluon plasma (QGP) formation [1]. The predicted enhancement of strangeness production in nucleus-nucleus collisions relative to proton-proton reactions was established experimentally some time ago [2, 3] and it was also found that this enhancement is increasing with the strangeness content of the particle type [6]. However, a clear interpretation of these phenomena requires a systematic investigation of the energy and system size dependence of strangeness production. In the following we report on some aspects of such a study done by the NA49 experiment.

II. ENERGY DEPENDENCE

Figure 1 shows a comparison of the energy dependence of mid-rapidity Λ , $\bar{\Lambda}$, Ξ^- , and $\bar{\Xi}^+$ production to several models and results from other experiments. While the transport models UrQMD1.3 and HSD provide a reasonable description of the Λ/π and $\bar{\Lambda}/\pi$ ratios, they are clearly below the data points in case of the Ξ^- and $\bar{\Xi}^+$. This might indicate that an addi-

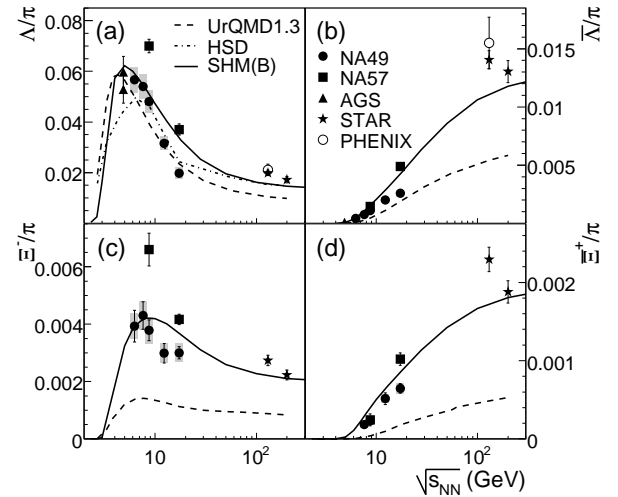


FIG. 1: The rapidity densities dN/dy at mid-rapidity of Λ (a), $\bar{\Lambda}$ (b), Ξ^- (c), and $\bar{\Xi}^+$ (d) divided by the pion rapidity densities ($\pi = 1.5(\pi^+ + \pi^-)$) in central Pb+Pb and Au+Au collisions as a function of $\sqrt{s_{NN}}$ [4]. The systematic errors are represented by the gray boxes. Also shown are NA57 [5, 6], AGS [7, 8, 9, 10], and RHIC [11, 12, 13, 14, 15, 16, 17] data, as well as calculations with hadronic transport models (HSD, UrQMD1.3 [18, 19, 20]) and a statistical hadron gas model (SHM(B) [21]).

tional partonic contribution is necessary to reach the production rates observed for multi-strange particles. Statistical models on the other hand generally provide a better match to the data. These models are based on the assumption that the particle yields correspond to their chemical

*Electronic address: blume@ikf.uni-frankfurt.de

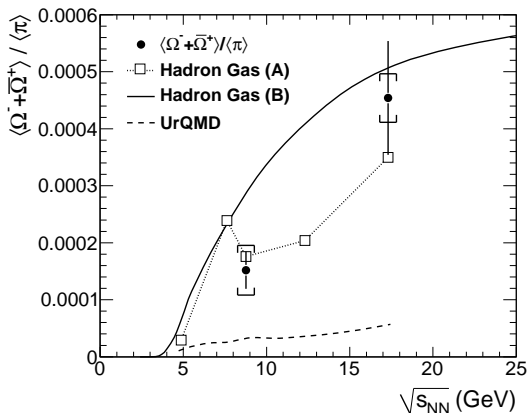


FIG. 2: The total yield of $\Omega^- + \bar{\Omega}^+$ divided by the total number of pions $\langle \pi \rangle$ ($\langle \pi \rangle = 1.5 (\pi^+ + \pi^-)$) versus the center-of-mass energy [22]. The dashed curve shows the prediction from the hadronic transport model UrQMD1.3 [19]. A hadron gas model without strangeness suppression [24] is shown by the full curve. The open squares represent the fits from [23] including a strangeness under-saturation factor γ_s .

equilibrium value and can thus be described by the parameters temperature T , baryonic chemical potential μ_B , volume V , and, in some implementations, by an additional strangeness under-saturation factor γ_s . The curves shown in Fig. 1 labeled SHM(B) are taken from [21] and are based on parametrizations of the $\sqrt{s_{NN}}$ dependence of T and μ_B .

The difference between the two model approaches discussed here is even more prominent for the Ω , as demonstrated in Fig. 2. In this case the deviation to the hadronic transport model is of the order of a factor of 10, while both the statistical model approaches shown in Fig. 2 are quite close to the data points.

While multi-strange hyperons generally seem to be close to the full equilibrium expectation at all energies, the ϕ -meson exhibits significant discrepancies (see Fig. 3). While at lower energies the ϕ production is close to both, the statistical model and the transport model UrQMD1.3, at top SPS energies none of the models does match the measurements. Please note that the apparent discrepancy of UrQMD1.3 with the ϕ/π ratios at lower energies, as visible in Fig. 3, is rather due to an overestimate of the pion yields and not an underestimate of the ϕ yields [25]. Also shown in Fig. 3 is a measurement of the ϕ

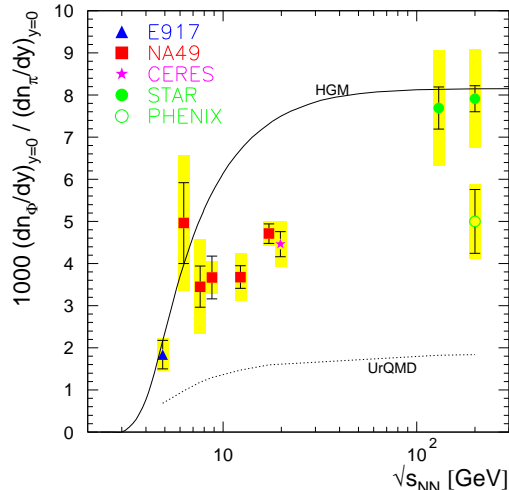


FIG. 3: The rapidity densities dN/dy at mid-rapidity of ϕ divided by the pion rapidity densities ($\pi = 1.5(\pi^+ + \pi^-)$) in central nucleus-nucleus collisions as a function of $\sqrt{s_{NN}}$ [25]. Also shown are NA45/CERES [26], and RHIC [27, 28] data, as well as calculations with hadronic transport models (UrQMD1.3 [19]) and a statistical hadron gas model (HGM [21]).

yields via the dielectron decay $\phi \rightarrow e^+ + e^-$ performed by the NA45 collaboration at 158A GeV [26]. This result agrees quite well with the NA49 result, which has been measured using the hadronic decay branch $\phi \rightarrow K^+ + K^-$.

III. SYSTEM SIZE DEPENDENCE

The system size dependence of Λ , $\bar{\Lambda}$, and Ξ^- production close to mid-rapidity, as measured at SPS energies, is summarized in Fig. 4. For Λ and $\bar{\Lambda}$ a relatively early saturation at $\langle N_w \rangle \approx 60$ is observed by NA49. However, a clear discrepancy between the data of NA49 and NA57 is still present. The transport models UrQMD2.3 [30] and HSD [18] are close to the data points for Λ , but are slightly below the $\bar{\Lambda}$ measurements. The Ξ^- production is clearly under-predicted at all system sizes. The core-corona approach [31, 32] provides generally a much better description of the system size dependence of all strange particle species. Here the relevant quantity is the fraction of nucleons that scatter more than once $f(\langle N_w \rangle)$ which can be calculated in a Glauber model. This allows for an interpolation between the yields Y

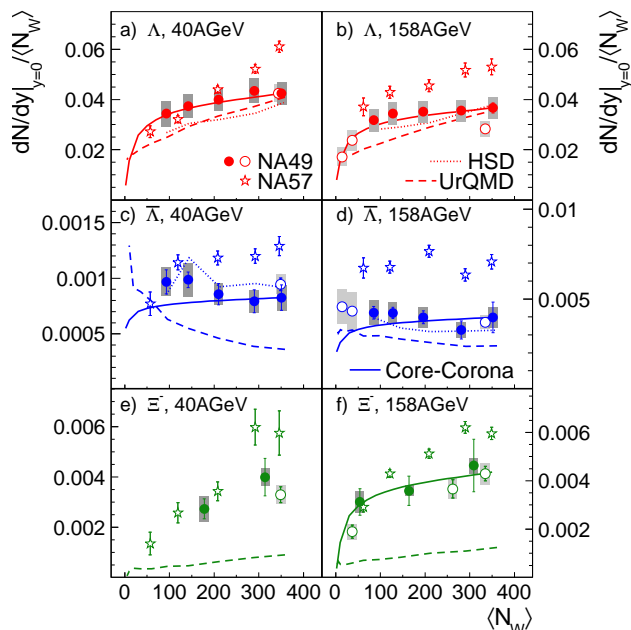


FIG. 4: The rapidity densities dN/dy divided by the average number of wounded nucleons $\langle N_w \rangle$ of Λ , $\bar{\Lambda}$, and Ξ^- at mid-rapidity for Pb+Pb collisions at 40A and 158A GeV, as well as for near-central C+C and Si+Si reactions at 158A GeV, as a function of $\langle N_w \rangle$ [29]. Also shown are data of the NA57 collaboration [5, 6] (open stars) and calculations with the HSD model [18] (dotted lines), the UrQMD2.3 model [19, 30] (dashed lines), and the core-corona approach (solid lines) [31, 32].

measured in elementary p+p ($= Y_{\text{corona}}$) and in central nucleus-nucleus collisions ($= Y_{\text{core}}$):

$$Y(\langle N_w \rangle) = \langle N_w \rangle [f(\langle N_w \rangle) Y_{\text{core}} + (1 - f(\langle N_w \rangle)) Y_{\text{corona}}]$$

Please note that the curves shown in Fig. 4 and Fig. 5 are based on a function $f(\langle N_w \rangle)$ that was calculated for Pb+Pb interactions. Therefore their comparison to the smaller systems C+C and Si+Si is not directly possible, since their surface to volume ratio is different.

It is interesting to observe that this approach not only works for yields, but also for dynamical quantities such as $\langle m_t \rangle - m_0$ (see Fig. 5). This suggests that the core-corona picture provides in general a reasonable way for understanding the evolution from elementary p+p to central Pb+Pb collisions.

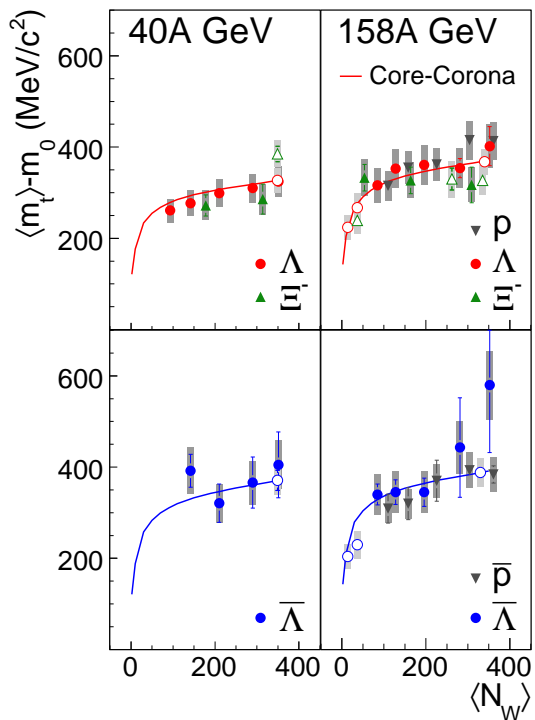


FIG. 5: The $\langle m_t \rangle - m_0$ values at mid-rapidity for Pb+Pb collisions at 40A and 158A GeV, as well as for near-central C+C and Si+Si reactions at 158A GeV [29]. The (anti-)proton data are taken from [33]. Also shown are the results from a fit for Λ and $\bar{\Lambda}$ with the core-corona approach (solid lines).

IV. RESONANCES

Strange resonances are of particular interest due to their short lifetimes that are in the same order as the lifetime of the fireball. Because of this their yields can still be modified after chemical freeze-out via destruction and regeneration mechanisms. For instance the particles resulting from the decay of such a resonance can rescatter in the fireball such that the resonance cannot be reconstructed any more. These effects can thus lead to deviations from the chemical equilibrium expectation.

New data on the $K^*(892)$ ($\bar{K}^*(892)$) production in central nucleus-nucleus collisions at 158A GeV are summarized in Fig. 6. The $K^*(892)$ ($\bar{K}^*(892)$) are reconstructed via the decay $K^*(892) \rightarrow K^+ + \pi^-$ ($\bar{K}^*(892) \rightarrow K^- + \pi^+$). As shown in the upper panel of Fig. 6, the sys-

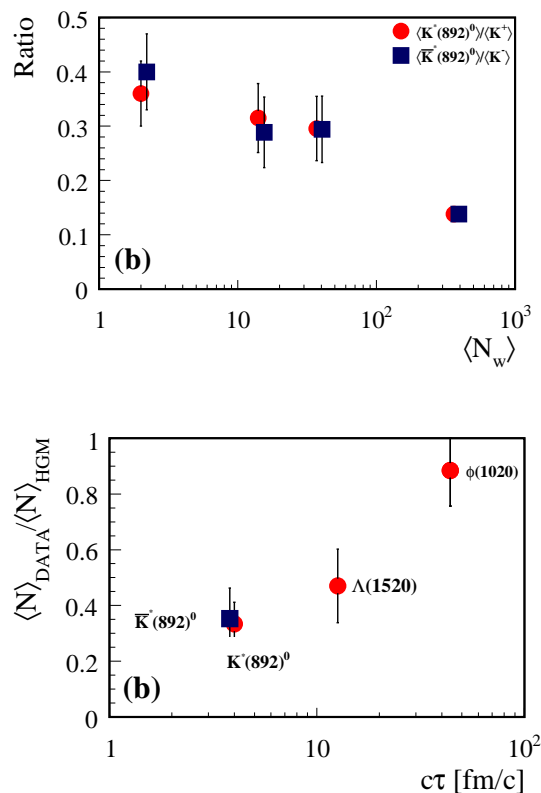


FIG. 6: Upper panel: The total yield of $K^*(892)$ ($\bar{K}^*(892)$) divided by the total yields of K^+ (K^-) in p+p and nucleus-nucleus collisions at 158A GeV as a function of the average number of wounded nucleons $\langle N_w \rangle$. Lower panel: The total yield of $K^*(892)$ ($\bar{K}^*(892)$), $\Lambda(1520)$, and ϕ in central Pb+Pb collisions at 158A GeV divided by the expectation from a statistical model fit [34] as a function of the resonance lifetime $c\tau$.

tem size dependence of the total $K^*(892)$ yield is clearly different than the one of charged kaons, the ratios $K^*(892)/K^+$ ($\bar{K}^*(892)/K^-$) decrease with increasing system size. This could be indicative of a stronger reduction of the measurable $K^*(892)$ yields in the larger fireball of central Pb+Pb reactions compared to the smaller one produced in C+C and Si+Si collisions, because here their decay products have a higher probability of rescattering with the medium.

The lower panel of Fig. 6 compares the total yields of several resonances ($K^*(892)$, $\Lambda(1520)$, and ϕ) to the expectations from a statistical model fit [34]. The fit did not include the resonances themselves. The deviation is largest for the short lived $K^*(892)$, while it is slightly less pronounced for the $\Lambda(1520)$ and even less for the ϕ , which has a much longer lifetime than the other two resonances. Comparing the yields of resonances with different lifetimes can thus provide a means to study the time-like extension of the hot and dense fireball created in heavy ion reactions.

-
- [1] J. Rafelski and B. Müller, Phys. Rev. Lett. **48**, 1066 (1982).
[2] J. Bartke et al. (NA35 Collaboration), Z. Phys. C **48**, 191 (1990).
[3] T. Alber et al. (NA35 Collaboration), Z. Phys. C **64**, 195 (1994).
[4] C. Alt et al. (NA49 Collaboration), Phys. Rev. C **78**, 034918 (2008).
[5] F. Antinori et al. (NA57 Collaboration), Phys. Lett. B **595**, 68 (2004).
[6] F. Antinori et al. (NA57 Collaboration), J. Phys. G **32**, 427 (2006).
[7] S. Ahmad et al. (E891 Collaboration), Phys. Lett. B **382**, 35 (1996).
[8] S. Alfero et al. (E896 Collaboration), Phys. Rev. Lett. **88**, 062301 (2002).
We use the 4π extrapolation given in: F. Becattini et al., Phys. Rev. C **69**, 024905 (2004).
[9] B. B. Back et al. (E917 Collaboration), Phys. Rev. Lett. **87**, 242301 (2001).
[10] L. Ahle et al. (E802 Collaboration), Phys. Rev. C **57**, R466 (1998).
[11] C. Adler et al. (STAR Collaboration), Phys. Rev. Lett. **89**, 092301 (2002).
[12] J. Adams et al. (STAR Collaboration), Phys. Rev. Lett. **92**, 182301 (2004).
[13] J. Adams et al. (STAR Collaboration), Phys. Lett. B **382**, 35 (1996).
S. Ahmad et al., Nucl. Phys. A **636**, 507 (1998).

- Rev. Lett. **98**, 062301 (2007).
- [14] C. Adler et al. (STAR Collaboration), Phys. Lett. B **595**, 143 (2004).
- [15] J. Adams et al. (STAR Collaboration), Phys. Rev. Lett. **92**, 112301 (2004).
- [16] K. Adcox et al. (PHENIX Collaboration), Phys. Rev. Lett. **89**, 092302 (2002).
- [17] K. Adcox et al. (PHENIX Collaboration), Phys. Rev. Lett. **88**, 242301 (2002).
- [18] W. Cassing and E. L. Bratkovskaya, Phys. Rep. **308**, 65 (1999).
- [19] M. Bleicher et al., J. Phys. G **25**, 1859 (1999), and private communication.
- [20] E. L. Bratkovskaya et al., Phys. Rev. C **69**, 054907 (2004).
- [21] A. Andronic, P. Braun-Munzinger, and J. Stachel, Nucl. Phys. A **772**, 167 (2006) and private communication.
- [22] C. Alt et al. (NA49 Collaboration), Phys. Rev. Lett. **94**, 192301 (2005).
- [23] F. Becattini, M. Gaździcki, A. Keränen, J. Manninen, and R. Stock, Phys. Rev. C **69**, 024905 (2004).
- [24] P. Braun-Munzinger, J. Cleymans, H. Oeschler, and K. Redlich, Nucl. Phys. A **697**, 902 (2002) and private communication.
- [25] C. Alt et al. (NA49 Collaboration), Phys. Rev. C **78**, 044907 (2008).
- [26] D. Adamová et al. (NA45/CERES Collaboration), Phys. Rev. Lett. **96**, 152301 (2006).
- [27] J. Adams et al. (STAR Collaboration), Phys. Lett. B **612**, 181 (2005).
- [28] S.S. Adler et al. (PHENIX Collaboration), Phys. Rev. C **72**, 014903 (2005).
- [29] T. Anticic et al. (NA49 Collaboration), Phys. Rev. C **80**, 034906 (2009).
- [30] H. Petersen, M. Mitrovski, T. Schuster, and M. Bleicher, arXiv:0903.0396.
- [31] F. Becattini, and J. Manninen, J. Phys. G **35**, 104013 (2008).
F. Becattini and J. Manninen, Phys. Lett. B **673**, 19 (2009).
- [32] J. Aichelin and K. Werner, Phys. Rev. C **79**, 064907 (2009).
- [33] T. Anticic et al. (NA49 Collaboration), Phys. Rev. C **69**, 024902 (2004).
- [34] F. Becattini, J. Manninen, and M. Gaździcki, Phys. Rev. C **73**, 044905 (2006).